Instituto de Física Teórica UAM-CSIC
UAM Universidad Autónoma de Madrid
CSIC
MINISTERIO DE CIENCIA E INNOVACIÓN
Financiado por la Unión Europea NextGenerationEU
Plan de Recuperación, Transformación y Resiliencia
AGENCIA ESTATAL DE INVESTIGACIÓN

Gravitational Waves from Hidden Sectors

Particle Production in the Early Universe — CERN, Sept. 9–13, 2024

Eric Madge (IFT-UAM/CSIC)

based on: Breitbach et al., JCAP **07** (2019) 007
Banerjee et al., PRD **104** (2021) 5
Madge et al., SciPost Phys. **12** (2022) 5, 171
Madge et al., JHEP **10** (2023) 171
Caprini et al. (LISA CosWG), arXiv:2403.03723 [astro-ph.CO]

GWs from Hidden Sectors

[image credit: ChatGPT/DALL-E]

cosmological sources

inflation

bosonic instabilities

thermal fluctuations

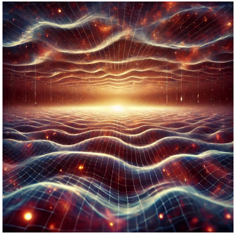

phase transitions

cosmic strings

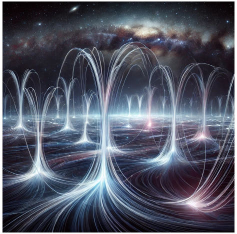

domain walls

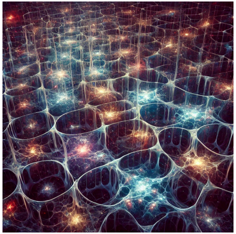

GWs from Hidden Sectors

[image credit: ChatGPT/DALL-E]

cosmological sources

inflation

bosonic instabilities

thermal fluctuations

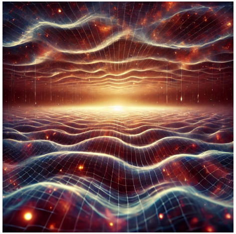

phase transitions

cosmic strings

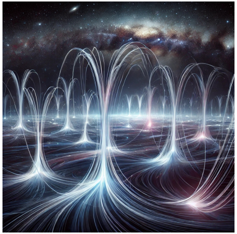

domain walls

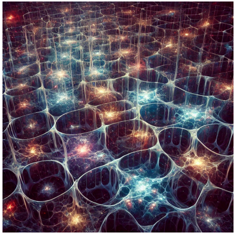

astrophysics

binary mergers

exotic objects

GWs from Hidden Sectors

[image credit: ChatGPT/DALL-E]

cosmological sources

inflation

bosonic instabilities

thermal fluctuations

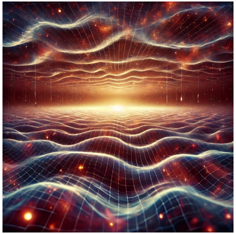

phase transitions

cosmic strings

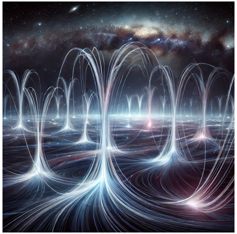

domain walls

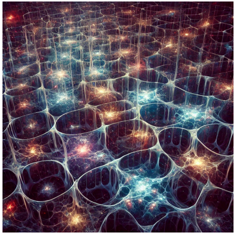

astrophysics

binary mergers

exotic objects

SGWB from Primordial Sources

peak frequency

set by characteristic scale f_*^{-1} at production: $f_*^{-1} \lesssim H_*^{-1}$

$\downarrow$

$$f_0 \sim \frac{a_0}{a_*} H_* \frac{f_*}{H_*}$$

$$\sim 0.1\,\mathrm{mHz} \left(\frac{T_*}{1\,\mathrm{TeV}}\right) \left(\frac{f_*}{H_*}\right)$$

SGWB from Primordial Sources

peak frequency

set by characteristic scale f_*^{-1} at production: $f_*^{-1} \lesssim H_*^{-1}$

↓

$$f_0 \sim \frac{a_0}{a_*} H_* \frac{f_*}{H_*}$$

$$\sim 0.1\,\mathrm{mHz} \left(\frac{T_*}{1\,\mathrm{TeV}}\right) \left(\frac{f_*}{H_*}\right)$$

peak amplitude

$$\rho_{\mathrm{GW}} \sim M_{\mathrm{pl}}^2 \langle \dot{h}_{ij} \dot{h}_{ij} \rangle, \quad \Box \bar{h}_{\mu\nu} \sim \frac{T_{\mu\nu}}{M_{\mathrm{pl}}^2}$$

↓

$$\Omega_{\mathrm{GW}} \sim \left(\frac{a_*}{a_0}\right)^4 \frac{1}{\rho_c} \frac{\rho^2_{\mathrm{source}}}{f_*^2 M_{\mathrm{pl}}^2}$$

$$\sim \left(\frac{a_*}{a_0}\right)^4 \left(\frac{H_0}{H_*}\right)^2 \left(\frac{H_*}{f_*}\right)^2 \Omega^2_{\mathrm{source}}$$

Cosmological Phase Transition

1. Cosmological Phase Transition
2. Bosonic Instabilities
3. Conclusions

Cosmological Phase Transitions

- thermal corrections typically restore spontaneously broken symmetries at high temperatures
  $\Longrightarrow$ symmetry breaking phase transition
- can be crossover or first-order

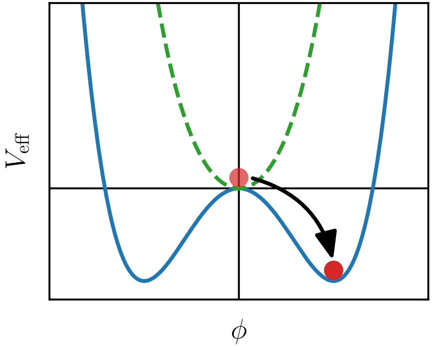

Cosmological Phase Transitions

- thermal corrections typically restore spontaneously broken symmetries at high temperatures
  $\Longrightarrow$ symmetry breaking phase transition
- can be crossover or first-order

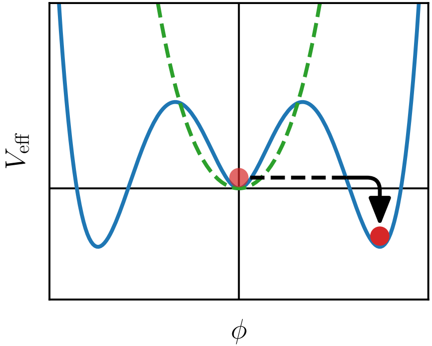

Cosmological Phase Transitions

- thermal corrections typically restore spontaneously broken symmetries at high temperatures
  $\Longrightarrow$ symmetry breaking phase transition
- can be crossover or first-order

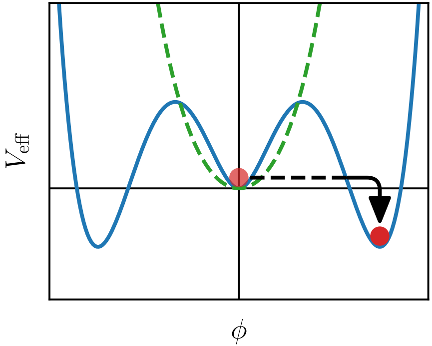

GW production:

1. vacuum bubble collisions

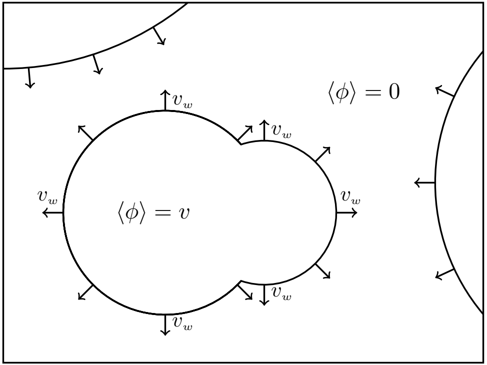

Cosmological Phase Transitions

- thermal corrections typically restore spontaneously broken symmetries at high temperatures
  $\Longrightarrow$ symmetry breaking phase transition
- can be crossover or first-order

GW production:

1. vacuum bubble collisions
2. sound waves collisions

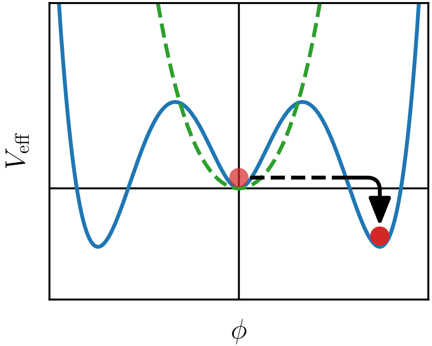

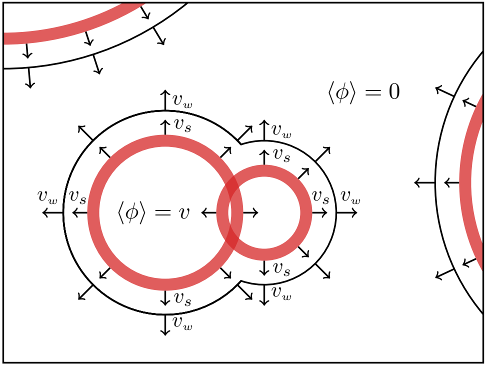

Cosmological Phase Transitions

- thermal corrections typically restore spontaneously broken symmetries at high temperatures
  $\Longrightarrow$ symmetry breaking phase transition
- can be crossover or first-order

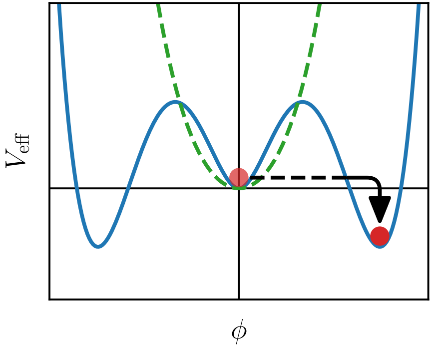

GW production:

1. vacuum bubble collisions
2. sound waves collisions
3. turbulence and vortical motion

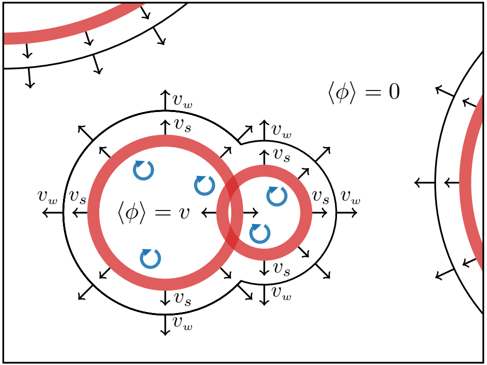

Phase Transition Parameters and Gravitational Wave Spectrum

Gravitational Wave spectrum obtained from numerical simulations and analytical arguments, expressed in terms of few parameters:

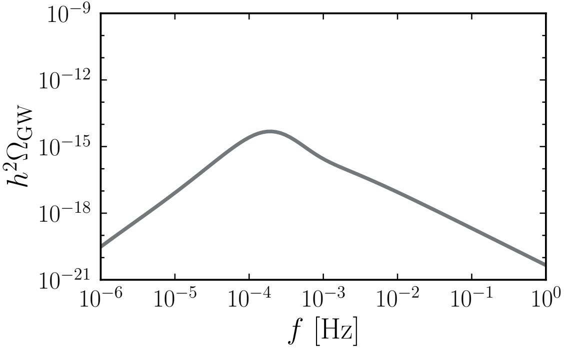

critical action: $S_{\rm crit} = \frac{1}{T}\int d^3x \left[\frac{1}{2}(\nabla\phi)^2 + V_{\rm eff}(\phi, T)\right]$

nucleation rate: $\Gamma(T) = A(T)\,\exp\left[-S_{\rm crit}(T)\right]$

Phase Transition Parameters and Gravitational Wave Spectrum

Gravitational Wave spectrum obtained from numerical simulations and analytical arguments, expressed in terms of few parameters:

strength/
energy budget

$$\alpha = \frac{\rho_{\text{vac}}}{\rho^*_{\text{rad}}} \simeq \frac{\Delta V_{\text{eff}}}{\rho^*_{\text{rad}}}$$

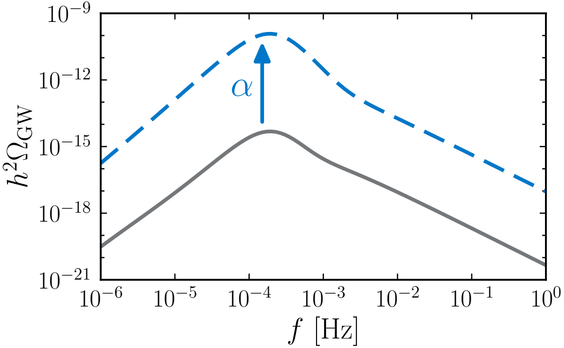

critical action: $S_{\text{crit}} = \frac{1}{T}\int \mathrm{d}^3x \left[\frac{1}{2}(\nabla\phi)^2 + V_{\text{eff}}(\phi, T)\right]$

nucleation rate: $\Gamma(T) = A(T)\,\exp\left[-S_{\text{crit}}(T)\right]$

Phase Transition Parameters and Gravitational Wave Spectrum

Gravitational Wave spectrum obtained from numerical simulations and analytical arguments, expressed in terms of few parameters:

strength/ energy budget

$$\alpha = \frac{\rho_{\rm vac}}{\rho^*_{\rm rad}} \simeq \frac{\Delta V_{\rm eff}}{\rho^*_{\rm rad}}$$

characteristic scale $\beta = \dot{\Gamma}/\Gamma$

$$\frac{\beta}{H_*} = \left[T \frac{dS_{\rm crit}}{{\rm d}T} \right]_{T=T_*}$$

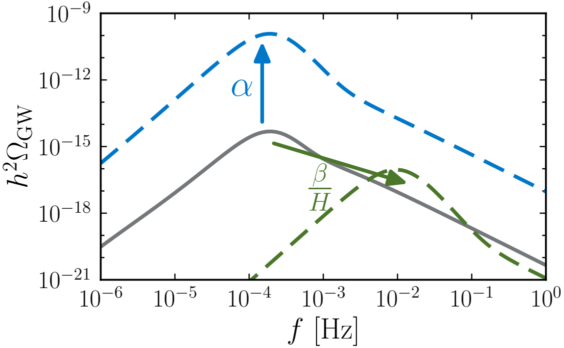

critical action: $S_{\rm crit} = \frac{1}{T} \int {\rm d}^3x \left[\frac{1}{2}(\nabla\phi)^2 + V_{\rm eff}(\phi, T) \right]$

nucleation rate: $\Gamma(T) = A(T)\, \exp\left[-S_{\rm crit}(T) \right]$

Phase Transition Parameters and Gravitational Wave Spectrum

Gravitational Wave spectrum obtained from numerical simulations and analytical arguments, expressed in terms of few parameters:

strength/ energy budget
$$\alpha = \frac{\rho_{\rm vac}}{\rho^*_{\rm rad}} \simeq \frac{\Delta V_{\rm eff}}{\rho^*_{\rm rad}}$$

characteristic scale $\beta = \dot{\Gamma}/\Gamma$
$$\frac{\beta}{H_*} = \left[T \frac{dS_{\rm crit}}{{\rm d}T} \right]_{T=T_*}$$

transition temperature
$$T_* \simeq T_n \quad \left(\Gamma(T_n) \simeq [H(T_n)]^4 \right)$$

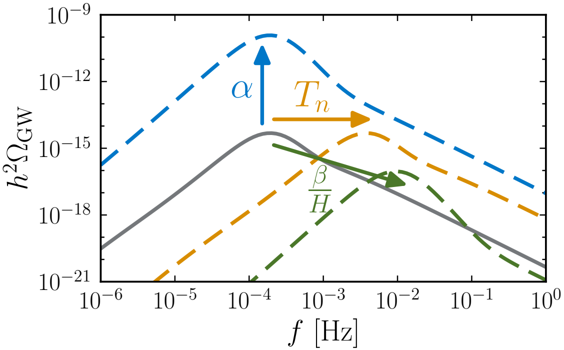

critical action: $S_{\rm crit} = \frac{1}{T} \int {\rm d}^3x \left[\frac{1}{2}(\nabla\phi)^2 + V_{\rm eff}(\phi, T) \right]$

nucleation rate: $\Gamma(T) = A(T)\, \exp\left[-S_{\rm crit}(T) \right]$

Phase Transition Parameters and Gravitational Wave Spectrum

Gravitational Wave spectrum obtained from numerical simulations and analytical arguments, expressed in terms of few parameters:

strength/ energy budget $\qquad \alpha = \dfrac{\rho_{\rm vac}}{\rho^*_{\rm rad}} \simeq \dfrac{\Delta V_{\rm eff}}{\rho^*_{\rm rad}}$

characteristic scale $\beta = \dot{\Gamma}/\Gamma$ $\qquad \dfrac{\beta}{H_*} = \left[T \dfrac{dS_{\rm crit}}{{\rm d}T} \right]_{T=T_*}$

transition temperature $\qquad T_* \simeq T_n \quad \left(\Gamma(T_n) \simeq [H(T_n)]^4\right)$

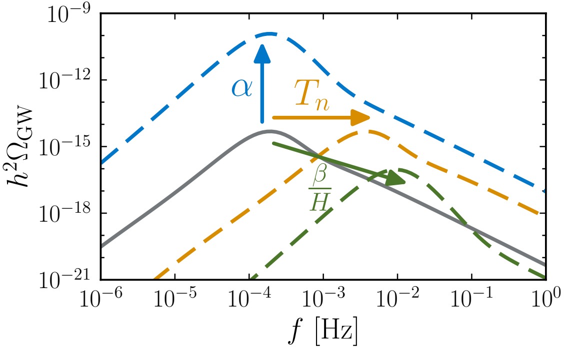

also: bubble dynamics:

wall velocity, efficiency factors, etc.

critical action: $\quad S_{\rm crit} = \frac{1}{T} \int {\rm d}^3x \left[\frac{1}{2}(\nabla\phi)^2 + V_{\rm eff}(\phi, T) \right]$

nucleation rate: $\quad \Gamma(T) = A(T)\, \exp\left[-S_{\rm crit}(T) \right]$

Decoupled Hidden Sectors

- sub-MeV hidden sectors contribute to the effective number of neutrino species N_{eff}

$$\rho_{\text{rad}} = \frac{\pi^2}{30} \sum_i g_i T_i^4 = \left[1 + \frac{7}{8} \left(\frac{4}{11}\right)^{\frac{4}{3}} N_{\text{eff}}\right] \rho_\gamma$$

- at $T \lesssim$ MeV:
additional relativistic DOFs in thermal equilibrium with photons are excluded

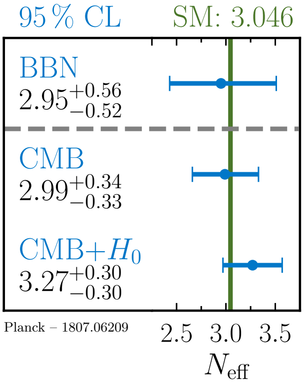

Decoupled Hidden Sectors

- sub-MeV hidden sectors contribute to the effective number of neutrino species N_{eff}

$$\rho_{\text{rad}} = \frac{\pi^2}{30} \sum_i g_i T_i^4 = \left[1 + \frac{7}{8}\left(\frac{4}{11}\right)^{\frac{4}{3}} N_{\text{eff}}\right] \rho_\gamma$$

- at $T \lesssim$ MeV:
additional relativistic DOFs in thermal equilibrium with photons are excluded

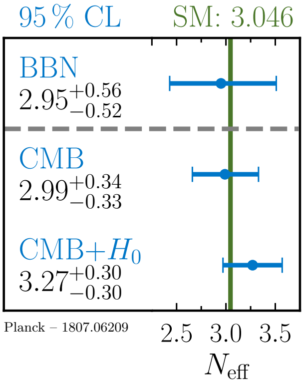

$\Longrightarrow$ sub-MeV hidden sector must be colder than SM

Hidden Sector Cosmology

completely decoupled

$$\xi_h \equiv \frac{T_h}{T_\gamma} < 1$$

$$N_{\text{eff}} = N_{\text{eff}}^{\text{SM}} + \frac{4}{7}\left(\frac{11}{4}\right)^{\frac{4}{3}} g_h\, \xi_h^4$$

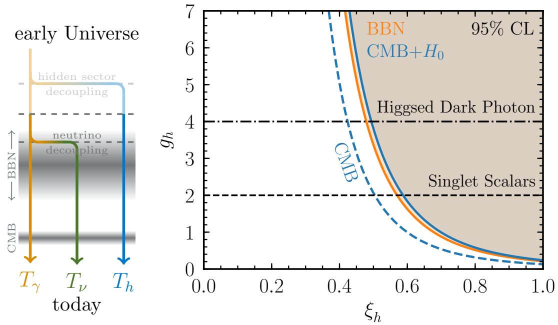

Hidden Sector Cosmology

Breitbach et al. (JCAP, 2019)

completely decoupled

$$\xi_h \equiv \frac{T_h}{T_\gamma} < 1$$

$$N_{\text{eff}} = N_{\text{eff}}^{\text{SM}} + \frac{4}{7}\left(\frac{11}{4}\right)^{\frac{4}{3}} g_h\, \xi_h^4$$

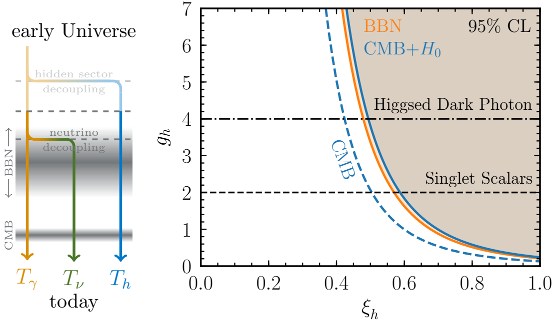

ν-quilibration

$$N_{\text{eff}} = \overbrace{\underbrace{N_{\text{eff}}^{\text{SM}}\left[1 + \frac{g_h}{g_\nu}\left(\xi_h^{\text{init}}\right)^4\right]}_{\text{BBN}}\left[1 + \frac{g_h}{g_\nu}\right]^{\frac{1}{3}}}^{\text{CMB}}$$

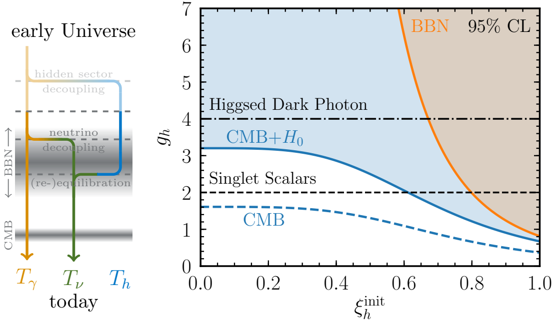

Phase Transitions in Secluded Hidden Sectors

temperature ratio: $\xi_h \equiv \dfrac{T_h}{T_\gamma}$

- $\alpha \simeq \alpha_h \, \xi_h^4$ $\qquad \alpha_h \equiv [\alpha]_{\xi_h=1}$
- $f^0_{\rm peak} \sim T_{n,\gamma} = \dfrac{T_{n,h}}{\xi_h}$
- $\dfrac{\beta}{H}$ ξ_h-independent

Phase Transitions in Secluded Hidden Sectors

Breitbach et al. (JCAP, 2019)
Fairbairn et al. (JHEP, 2019)

temperature ratio: $\xi_h \equiv \dfrac{T_h}{T_\gamma}$

- $\alpha \simeq \alpha_h \, \xi_h^4$ $\qquad \alpha_h \equiv [\alpha]_{\xi_h=1}$
- $f^0_{\rm peak} \sim T_{n,\gamma} = \dfrac{T_{n,h}}{\xi_h}$
- $\dfrac{\beta}{H}$ ξ_h-independent

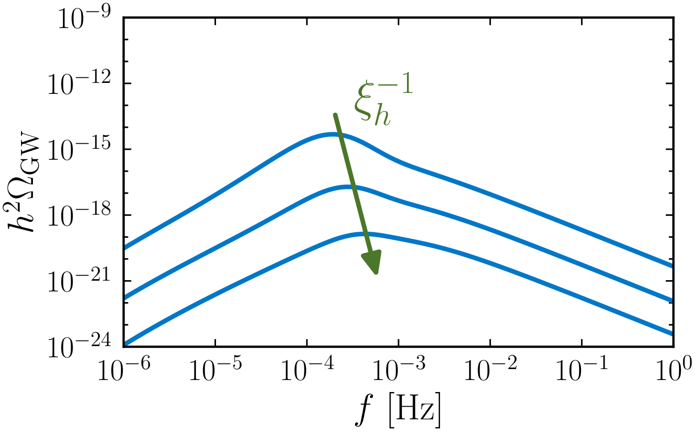

Sensitivity

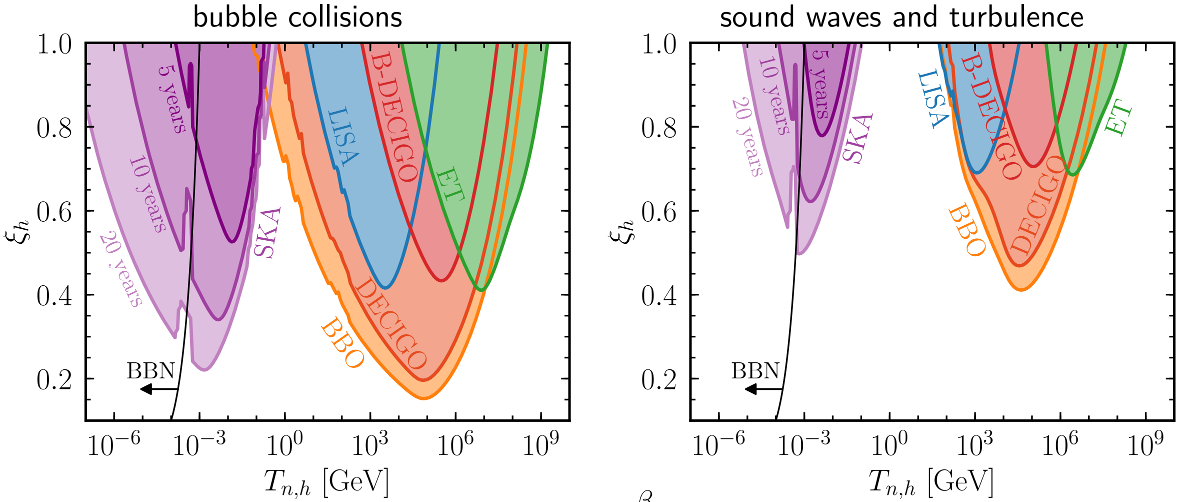

$$\alpha_h = 0.1, \quad \frac{\beta}{H_*} = 10$$

Parameter Reconstruction

Caprini et al. arXiv:2403.03723 [astro-ph.Co]
Lewicki et al. (JHEP, 2022); Ellis et al. (JHEP, 2023)
SGWBinner: Caprini et al. (JCAP, 2019); Flauger et al. (JCAP, 2021)

example: singlet w/ $\mathbb{Z}_2$ symmetry

$$\Delta\mathcal{L} = -\frac{\mu_s^2}{2}\, s^2 - \frac{\lambda_s}{4}\, s^4 - \frac{\lambda_{hs}}{2}\, s^2 H^\dagger H$$

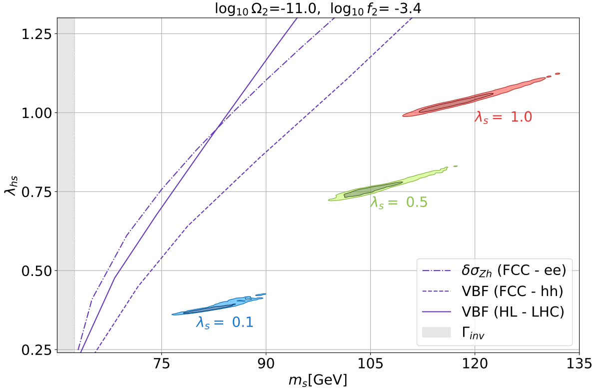

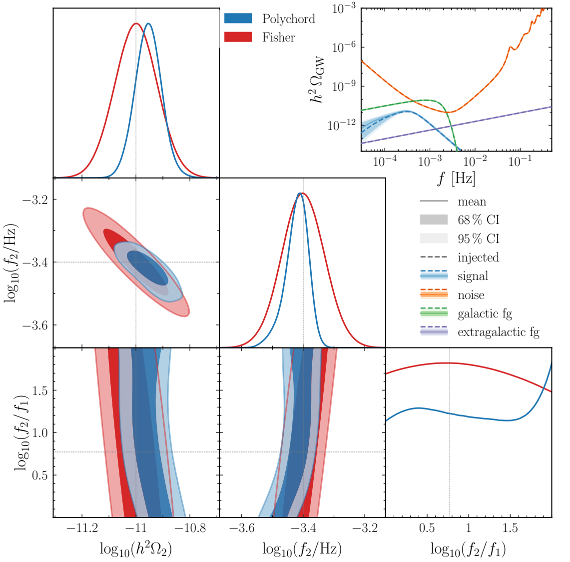

Bosonic Instabilities

Bosonic Instabilities: Audible Axions

Misaligment Mechanism

$$\mathcal{L} \supset \frac{1}{2}\partial_\mu\phi\partial^\mu\phi - V(\phi)$$

$$\Longrightarrow \qquad \ddot{\phi} + 3H\dot{\phi} + m_a^2\phi = 0$$

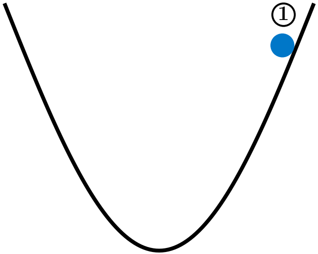

1. $H \gg m_a$: axion pinned by Hubble friction.

Bosonic Instabilities: Audible Axions

Misaligment Mechanism

$$\mathcal{L} \supset \frac{1}{2}\partial_\mu\phi\partial^\mu\phi - V(\phi)$$

$$\implies \qquad \ddot{\phi} + 3H\dot{\phi} + m_a^2\phi = 0$$

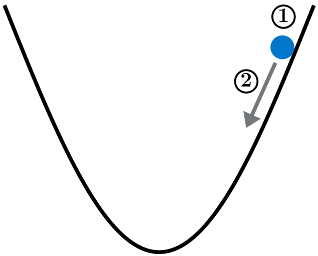

1. $H \gg m_a$: axion pinned by Hubble friction.
2. $H \sim m_a$: axion starts to roll

Bosonic Instabilities: Audible Axions

Machado et al. (JHEP 2019, PRD 2020)
Ratzinger et al. (SciPost Phys. 2021)

Misaligment Mechanism

$$\mathcal{L} \supset \frac{1}{2}\partial_\mu\phi\partial^\mu\phi - V(\phi)$$

$$\Longrightarrow \qquad \ddot{\phi} + 3H\dot{\phi} + m_a^2\phi = 0$$

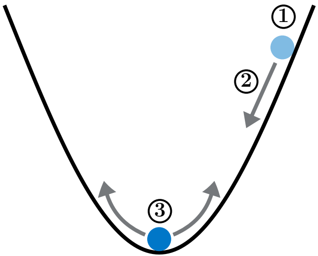

1. $H \gg m_a$: axion pinned by Hubble friction.
2. $H \sim m_a$: axion starts to roll
3. $H \ll m_a$: axion oscillates

Bosonic Instabilities: Audible Axions

Machado et al. (JHEP 2019, PRD 2020)
Ratzinger et al. (SciPost Phys. 2021)

Misaligment Mechanism + coupling to dark photon

$$\mathcal{L} \supset \frac{1}{2}\partial_\mu\phi\partial^\mu\phi - V(\phi) - \frac{1}{4}X_{\mu\nu}X^{\mu\nu} - \frac{\alpha}{4}\frac{\phi}{f_a}X_{\mu\nu}\tilde{X}^{\mu\nu}$$

$$\Longrightarrow \qquad \ddot{\phi} + 3H\dot{\phi} + m_a^2\phi = -\frac{\alpha}{f_a}\langle X_{\mu\nu}\tilde{X}^{\mu\nu}\rangle$$

e.g. to deplete axion abundance
Agrawal et al. (JHEP, 2018)
Kitajima et al. (PLB 2018)
or for dark-photon dark-matter
Dror et al. (PRD 2019)
Co et al. (PRD 2019)
Bastero-Gil et al. (JCAP 2019)
Agrawal et al. (PLB 2019)

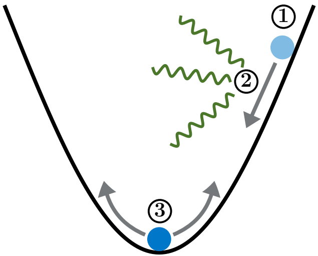

1. $H \gg m_a$: axion pinned by Hubble friction.
2. $H \sim m_a$: axion starts to roll
3. $H \ll m_a$: axion oscillates

$\Longrightarrow$ dark photon production during phase 2 (and 3)

Bosonic Instabilities: Audible Axions

Machado et al. (JHEP 2019, PRD 2020)
Ratzinger et al. (SciPost Phys. 2021)

Misaligment Mechanism $+$ coupling to dark photon

$$\mathcal{L} \supset \frac{1}{2}\partial_\mu\phi\partial^\mu\phi - V(\phi) - \frac{1}{4}X_{\mu\nu}X^{\mu\nu} - \frac{\alpha}{4}\frac{\phi}{f_a}X_{\mu\nu}\tilde{X}^{\mu\nu}$$

$$\Longrightarrow \qquad \ddot{\phi} + 3H\dot{\phi} + m_a^2\phi = -\frac{\alpha}{f_a}\langle X_{\mu\nu}\tilde{X}^{\mu\nu}\rangle$$

e.g. to deplete axion abundance
Agrawal et al. (JHEP, 2018)
Kitajima et al. (PLB 2018)
or for dark-photon dark-matter
Dror et al. (PRD 2019)
Co et al. (PRD 2019)
Bastero-Gil et al. (JCAP 2019)
Agrawal et al. (PLB 2019)

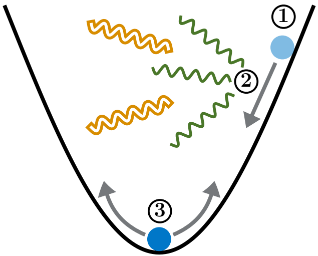

1. $H \gg m_a$: axion pinned by Hubble friction.
2. $H \sim m_a$: axion starts to roll
3. $H \ll m_a$: axion oscillates

$\Longrightarrow$ dark photon production during phase 2 (and 3)

$\Longrightarrow$ gravitational wave emission from dark photons

Dark Photon Production

dark photon EoM: $$X''_\pm(\tau,k) + \omega^2_\pm(k) X_\pm(\tau,k) = 0 \qquad \omega^2_\pm(k) = \left(k^2 \mp k\frac{\alpha\phi'(\tau)}{f_a}\right)$$

- modes with $k < \left|\frac{\alpha\phi'(\tau)}{f_a}\right|$ experience tachyonic instability in one helicity

Dark Photon Production

dark photon EoM: $$X''_{\pm}(\tau, k) + \omega^2_{\pm}(k) X_{\pm}(\tau, k) = 0 \qquad \omega^2_{\pm}(k) = \left(k^2 \mp k \frac{\alpha \phi'(\tau)}{f_a}\right)$$

- modes with $k < \left|\frac{\alpha \phi'(\tau)}{f_a}\right|$ experience tachyonic instability in one helicity
- largest growth for $\tilde{k} = \left|\frac{\alpha \phi'(\tau)}{2\, f_a}\right|$ with $\left|\omega^2(\tilde{k})\right| = \tilde{k}^2$

Dark Photon Production

dark photon EoM: $X''_\pm(\tau,k) + \omega^2_\pm(k) X_\pm(\tau,k) = 0$ $\quad \omega^2_\pm(k) = \left(k^2 \mp k \frac{\alpha\phi'(\tau)}{f_a}\right)$

- modes with $k < \left|\frac{\alpha\phi'(\tau)}{f_a}\right|$ experience tachyonic instability in one helicity
- largest growth for $\tilde{k} = \left|\frac{\alpha\phi'(\tau)}{2\, f_a}\right|$ with $\left|\omega^2(\tilde{k})\right| = \tilde{k}^2$
- for oscillating axion: $\tilde{k} \sim a^{-1/2}$

Dark Photon Production

dark photon EoM: $X''_\pm(\tau,k) + \omega^2_\pm(k) X_\pm(\tau,k) = 0$ $\qquad \omega^2_\pm(k) = \left(k^2 \mp k \frac{\alpha\phi'(\tau)}{f_a}\right)$

- modes with $k < \left|\frac{\alpha\phi'(\tau)}{f_a}\right|$ experience tachyonic instability in one helicity
- largest growth for $\tilde{k} = \left|\frac{\alpha\phi'(\tau)}{2\,f_a}\right|$ with $\left|\omega^2(\tilde{k})\right| = \tilde{k}^2$
- for oscillating axion: $\tilde{k} \sim a^{-1/2}$
- tachyonic band closes when $|\omega(\tilde{k})| < a\, m_a$

  $\Longrightarrow \sim$ energy transfer stops

Dark Photon Production

dark photon EoM: $X''_{\pm}(\tau,k) + \omega^2_{\pm}(k) X_{\pm}(\tau,k) = 0$ $\quad \omega^2_{\pm}(k) = \left(k^2 \mp k \frac{\alpha\phi'(\tau)}{f_a}\right)$

- modes with $k < \left|\frac{\alpha\phi'(\tau)}{f_a}\right|$ experience tachyonic instability in one helicity
- largest growth for $\tilde{k} = \left|\frac{\alpha\phi'(\tau)}{2\,f_a}\right|$ with $\left|\omega^2(\tilde{k})\right| = \tilde{k}^2$
- for oscillating axion: $\tilde{k} \sim a^{-1/2}$
- tachyonic band closes when $|\omega(\tilde{k})| < a\, m_a$

  $\Longrightarrow \sim$ energy transfer stops

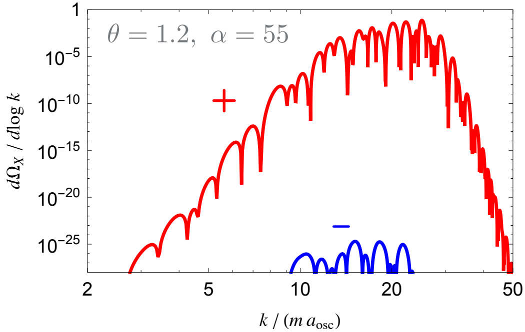

[Machado et al. (JHEP 2019)]

dark photon spectrum:

- peaked around $\tilde{k} \approx a_{\rm osc} m_a (\alpha\theta/2)^{2/3}$
- first tachyonic helicity dominates

Gravitational Wave Spectrum

GWs generated at t_* around the time when the tachyonic band closes:

- peak frequency:

$$f_{\mathsf{peak}} \sim 2\,\frac{\tilde{k}_*}{a_0} \sim 4\,\mathsf{nHz}\left(\frac{\alpha\,\theta}{100}\right)^{\frac{2}{3}}\left(\frac{m_a}{10^{-15}\,\mathsf{eV}}\right)^{\frac{1}{2}}$$

Gravitational Wave Spectrum

GWs generated at t_* around the time when the tachyonic band closes:

- peak frequency:

$$f_{\text{peak}} \sim 2\,\frac{\tilde{k}_*}{a_0} \sim 4\,\text{nHz}\left(\frac{\alpha\,\theta}{100}\right)^{\frac{2}{3}}\left(\frac{m_a}{10^{-15}\,\text{eV}}\right)^{\frac{1}{2}}$$

- peak amplitude:

$$\Omega_{\text{GW}}^{\text{peak}} \sim \frac{\left(\rho_X^*/f_{\text{peak}}^*\right)^2}{\rho_c\; M_{\text{pl}}^2}\left(\frac{a_*}{a_0}\right)^4 \sim 10^{-7}\left(\frac{f_a}{M_{\text{pl}}}\right)^4\left(100\,\frac{\theta^2}{\alpha}\right)^{\frac{4}{3}}$$

Gravitational Wave Spectrum

GWs generated at t_* around the time when the tachyonic band closes:

- peak frequency:

$$f_{\mathsf{peak}} \sim 2\,\frac{\tilde{k}_*}{a_0} \sim 4\,\mathsf{nHz}\left(\frac{\alpha\,\theta}{100}\right)^{\frac{2}{3}}\left(\frac{m_a}{10^{-15}\,\mathsf{eV}}\right)^{\frac{1}{2}}$$

- peak amplitude:

$$\Omega_{\mathsf{GW}}^{\mathsf{peak}} \sim \frac{\left(\rho_X^*/f_{\mathsf{peak}}^*\right)^2}{\rho_c\; M_{\mathsf{pl}}^2}\left(\frac{a_*}{a_0}\right)^4 \sim 10^{-7}\left(\frac{f_a}{M_{\mathsf{pl}}}\right)^4\left(100\,\frac{\theta^2}{\alpha}\right)^{\frac{4}{3}}$$

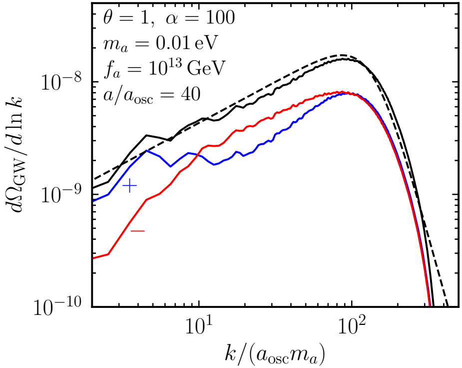

- spectral shape from lattice: [Ratzinger, Schwaller, Stefanek (SciPost Phys. 2022)]

$$\Omega_{\mathsf{GW}} = \Omega_{\mathsf{GW}}^{\mathsf{peak}}\,\mathcal{S}(f/f_{\mathsf{peak}}), \qquad \mathcal{S}(x) = x^{0.73}\left[\frac{1}{2}\left(1 + x^{4.2}\right)\right]^{\frac{-4.96-0.73}{4.2}}$$

Parameter Constraints

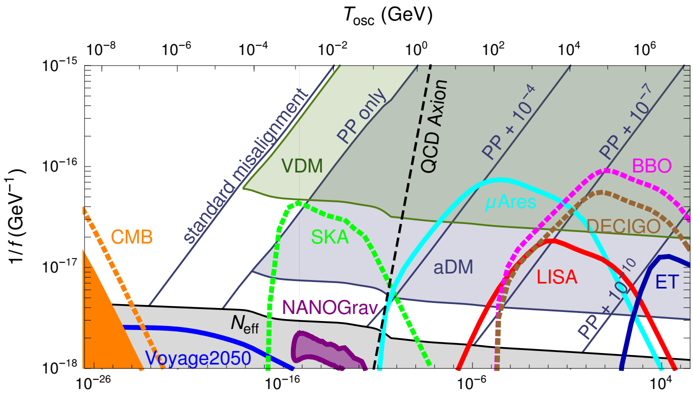

[Ratzinger et al. (SciPost Phys., 2022)]

Parameter Constraints

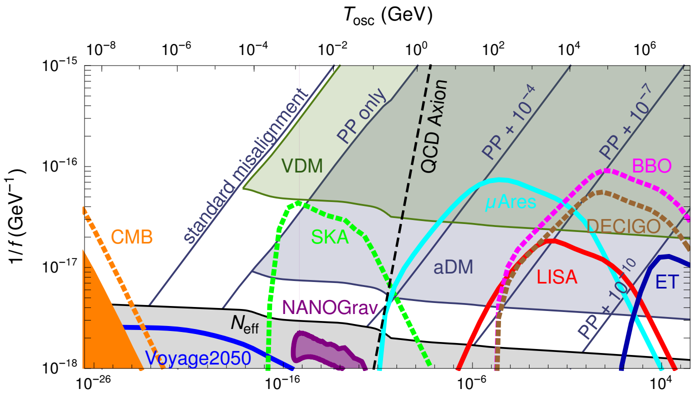

[Ratzinger et al. (SciPost Phys., 2022)]

[Madge et al. (JHEP 2023)]

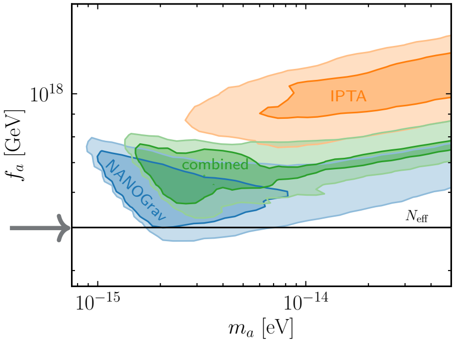

$$\Delta N_{\text{eff}} \sim 9.1 \left(\frac{\theta\, f_a}{M_{\text{pl}}}\right)^2$$

(also: $\Omega_a > \Omega_{\text{DM}}$)

Kinetic Misalignment

Co, Harigaya (PRL, 2020)
Co et al. (PRL, 2020)

misalignment + large initial velocity $\Longrightarrow$ DM abundance and GW amplitude set by $\dot{\phi}_0$

- complex scalar P with $V(P) \sim |P|^4$ and initial displacement $|P| \gg f_a$

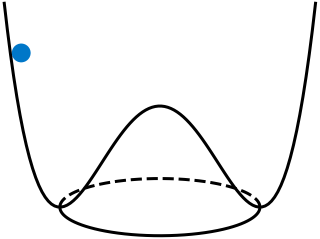

Kinetic Misalignment

Co, Harigaya (PRL, 2020)
Co et al. (PRL, 2020)

misalignment + large initial velocity $\Longrightarrow$ DM abundance and GW amplitude set by $\dot{\phi}_0$

- complex scalar P with $V(P) \sim |P|^4$ and initial displacement $|P| \gg f_a$
- high-dim. PQ breaking: $\Delta V_{\not{PQ}} \propto P^n + \text{h.c.}$ $\Longrightarrow$ angular motion

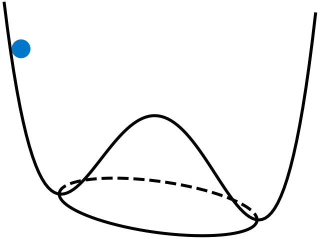

Kinetic Misalignment

Co, Harigaya (PRL, 2020)
Co et al. (PRL, 2020)

misalignment + large initial velocity $\Longrightarrow$ DM abundance and GW amplitude set by $\dot{\phi}_0$

- complex scalar P with $V(P) \sim |P|^4$ and initial displacement $|P| \gg f_a$
- high-dim. PQ breaking: $\Delta V_{\not{PQ}} \propto P^n + \text{h.c.}$ $\Longrightarrow$ angular motion
- PQ restored as $|P|$ decreases $\Longrightarrow$ circular motion

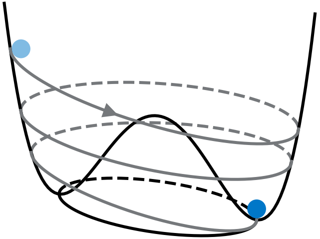

Kinetic Misalignment

Co, Harigaya (PRL, 2020)
Co et al. (PRL, 2020)

misalignment + large initial velocity $\Longrightarrow$ DM abundance and GW amplitude set by $\dot{\phi}_0$

- complex scalar P with $V(P) \sim |P|^4$ and initial displacement $|P| \gg f_a$
- high-dim. PQ breaking: $\Delta V_{\not{PQ}} \propto P^n + \text{h.c.}$ $\Longrightarrow$ angular motion
- PQ restored as $|P|$ decreases $\Longrightarrow$ circular motion

$\Longrightarrow$ dark photon and graviational wave production

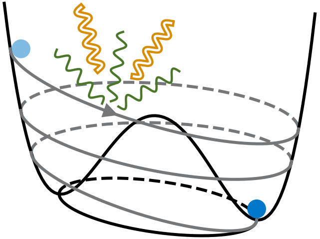

Kinetic Misalignment

Co, Harigaya (PRL, 2020)
Co et al. (PRL, 2020)

misalignment + large initial velocity $\Longrightarrow$ DM abundance and GW amplitude set by $\dot{\phi}_0$

- complex scalar P with $V(P) \sim |P|^4$ and initial displacement $|P| \gg f_a$
- high-dim. PQ breaking: $\Delta V_{\not{PQ}} \propto P^n + \text{h.c.}$ $\Longrightarrow$ angular motion
- PQ restored as $|P|$ decreases $\Longrightarrow$ circular motion

$\Longrightarrow$ dark photon and graviational wave production

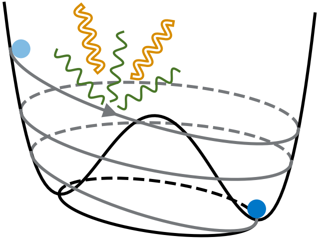

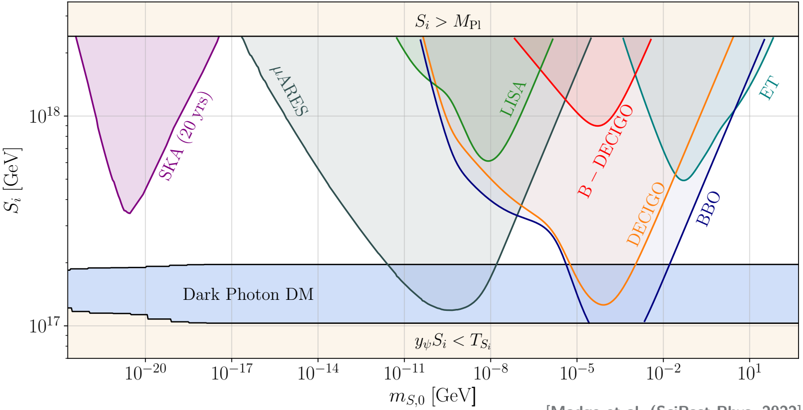

[Madge et al. (SciPost Phys. 2022)]

Relaxion

Graham et al. (PRL, 2015)

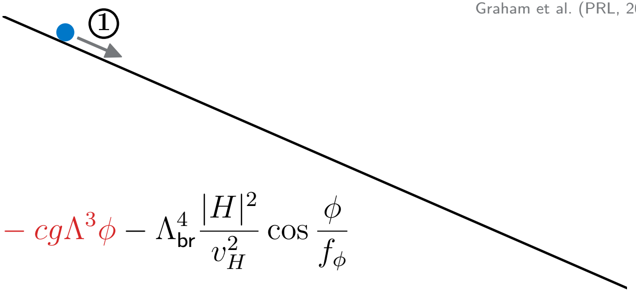

$$V(H,\phi) = \underbrace{\left(\Lambda^2 - g\Lambda\phi\right)}_{\mu_H^2(\phi)} |H|^2 + \lambda |H|^4 - cg\Lambda^3\phi - \Lambda_{\mathsf{br}}^4 \frac{|H|^2}{v_H^2} \cos\frac{\phi}{f_\phi}$$

1. $\mu_H^2 > 0$

Relaxion

Graham et al. (PRL, 2015)

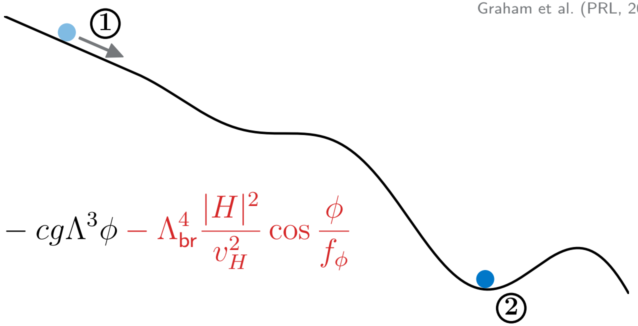

$$V(H,\phi) = \underbrace{\left(\Lambda^2 - g\Lambda\phi\right)}_{\mu_H^2(\phi)} |H|^2 + \lambda |H|^4 - cg\Lambda^3\phi - \Lambda_{\text{br}}^4 \frac{|H|^2}{v_H^2} \cos\frac{\phi}{f_\phi}$$

1. $\mu_H^2 > 0$
2. $\mu_H^2 < 0$

Relaxion

Graham et al. (PRL, 2015)

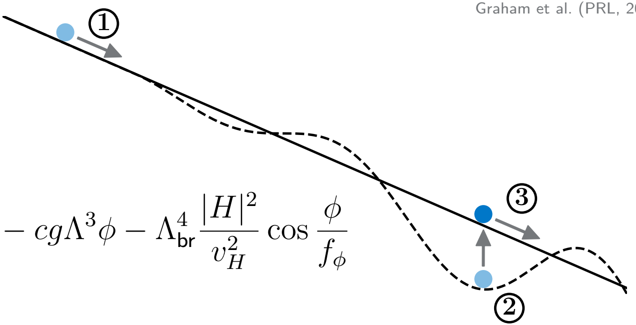

$$V(H,\phi) = \underbrace{\left(\Lambda^2 - g\Lambda\phi\right)}_{\mu_H^2(\phi)} |H|^2 + \lambda |H|^4 - cg\Lambda^3\phi - \Lambda_{\text{br}}^4 \frac{|H|^2}{v_H^2} \cos\frac{\phi}{f_\phi}$$

1. $\mu_H^2 > 0$
2. $\mu_H^2 < 0$
3. reheating

Relaxion

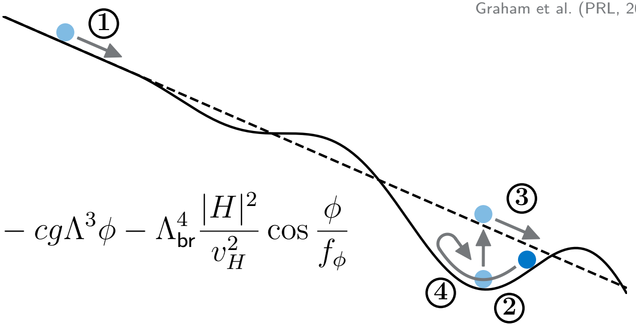

$$V(H,\phi) = \underbrace{\left(\Lambda^2 - g\Lambda\phi\right)}_{\mu_H^2(\phi)} |H|^2 + \lambda |H|^4 - cg\Lambda^3\phi - \Lambda_{\text{br}}^4 \frac{|H|^2}{v_H^2} \cos\frac{\phi}{f_\phi}$$

1. $\mu_H^2 > 0$
2. $\mu_H^2 < 0$
3. reheating
4. EWPT

Relaxion

Graham et al. (PRL, 2015)

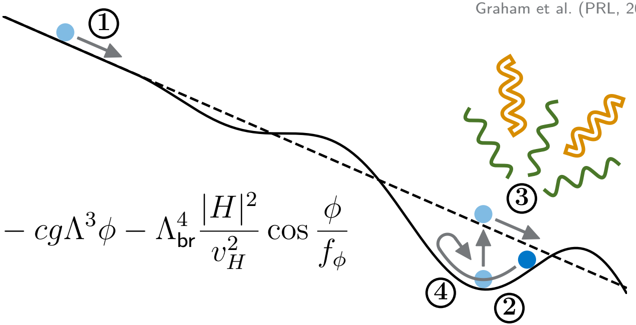

$$V(H,\phi) = \underbrace{\left(\Lambda^2 - g\Lambda\phi\right)}_{\mu_H^2(\phi)} |H|^2 + \lambda\,|H|^4 - cg\Lambda^3\phi - \Lambda_{\mathsf{br}}^4 \frac{|H|^2}{v_H^2} \cos\frac{\phi}{f_\phi}$$

1. $\mu_H^2 > 0$
2. $\mu_H^2 < 0$
3. reheating
4. EWPT

Relaxion

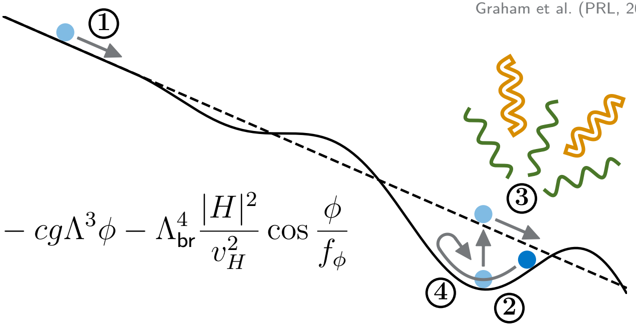

Graham et al. (PRL, 2015)

$$V(H,\phi) = \underbrace{\left(\Lambda^2 - g\Lambda\phi\right)}_{\mu_H^2(\phi)} |H|^2 + \lambda |H|^4 - cg\Lambda^3\phi - \Lambda_{\text{br}}^4 \frac{|H|^2}{v_H^2} \cos\frac{\phi}{f_\phi}$$

1. $\mu_H^2 > 0$
2. $\mu_H^2 < 0$
3. reheating
4. EWPT

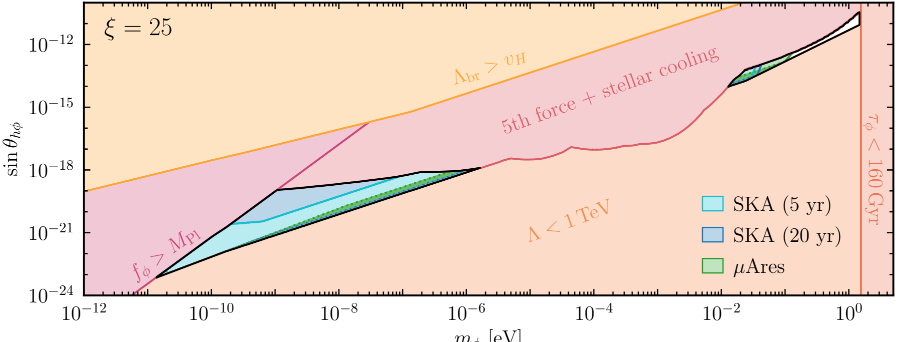

[Banerjee et al. (PRD, 2021)]

Conclusions

1. Cosmological Phase Transition
2. Bosonic Instabilities
3. Conclusions

Conclusion

- Hidden sectors can generate GWs in several ways
- The hidden sector can be decoupled

  $\Longrightarrow$ GW spectrum suppressed: $\quad f^0_{\text{peak}} \sim \xi_h, \quad \alpha \sim \xi_h^4$
- ALPs coupled to dark photons can produce SGWB via tachyonic instability

Thank you for your attention!

Gravitational Waves from Hidden Sectors

Particle Production in the Early Universe — CERN, Sept. 9–13, 2024

Eric Madge (IFT-UAM/CSIC)

backup slides

Hidden Sector Benchmark Models

Singlet Scalars:

- 2 real scalars S and A
- $\langle S \rangle = v_S\,,\ \langle A \rangle = 0$, A Z_2-odd

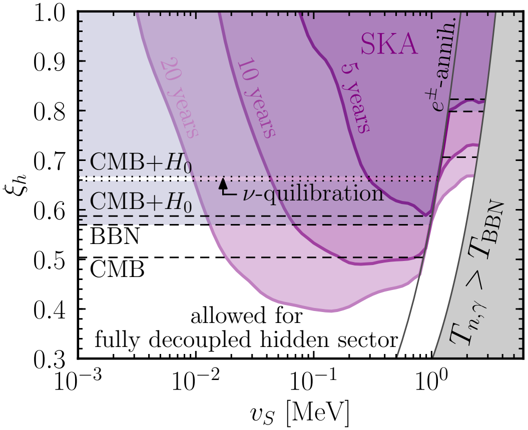

Dark Photon:

- complex SM singlet scalar
- charged under dark $U(1)_D$

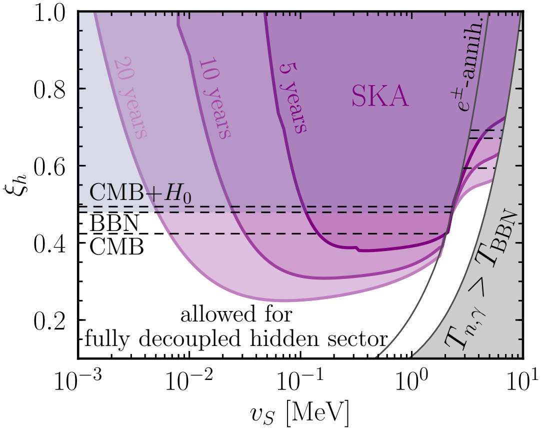

Hidden Sector Phase Transition Detectability

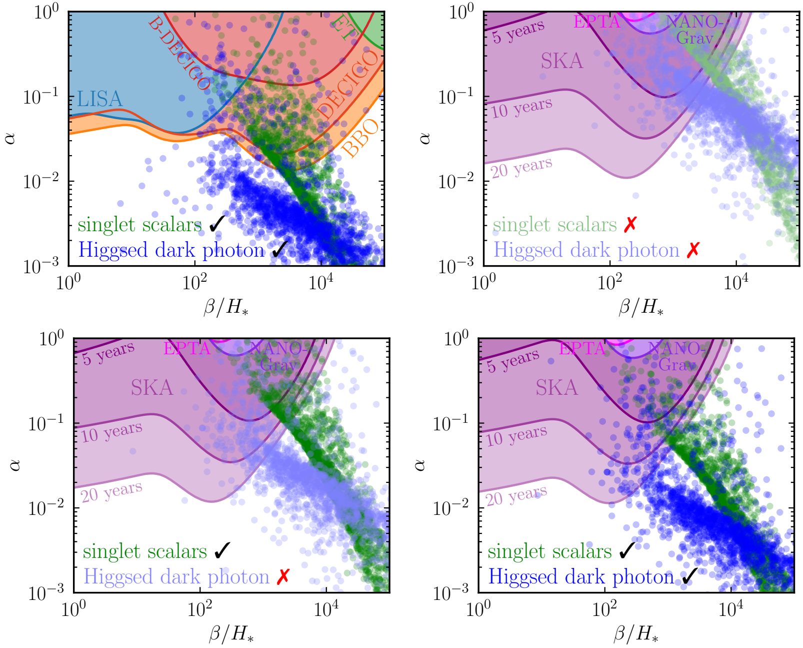

Audible Axion GW Spectrum

$f \ll f_{\text{peak}}$:

- unpolarized
- causality: $\sim f^3$

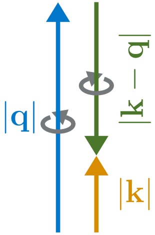

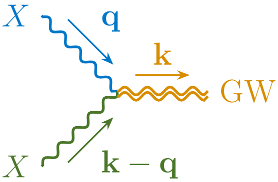

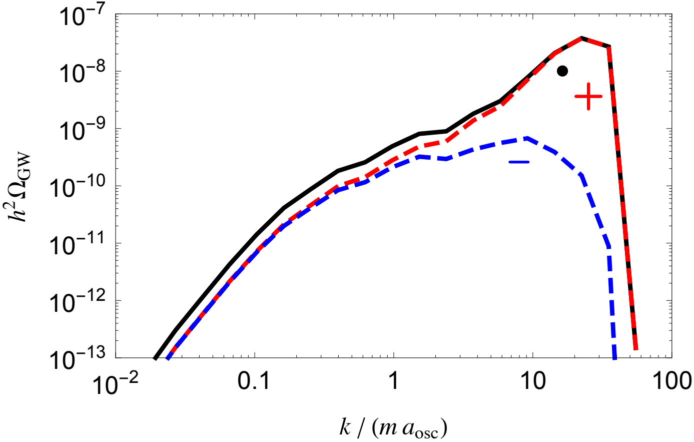

[Machado et al. (JHEP, 2019)]

$f \gg f_{\text{peak}}$:

- polarized
- $|\mathbf{k}-\mathbf{q}| > \tilde{k}_{\text{osc}}$
  $\Longrightarrow$ exp. supression

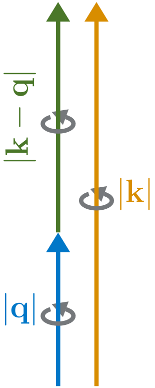

Dark Photon Production in Kinetic Misalignment

$$X''_\pm + \left(k^2 \mp k\frac{\alpha\phi'}{S}\right) X_\pm = 0$$

$$\Longrightarrow \tilde{k} = \frac{\alpha\phi'}{2S} \sim \begin{cases} \text{const.}, & S > f_\phi \\ a^{-2}, & S = f_\phi \end{cases}$$

- X production becomes efficient at $a = a_\star$ when $\tilde{k} > a_\star H_\star$
- backreaction on axion motion delayed until $a = a_{\mathsf{GW}}$ by X mode growth time

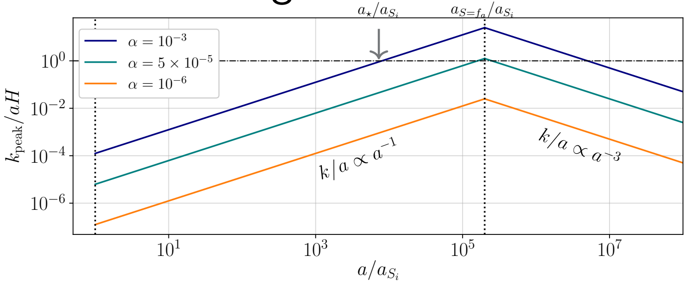

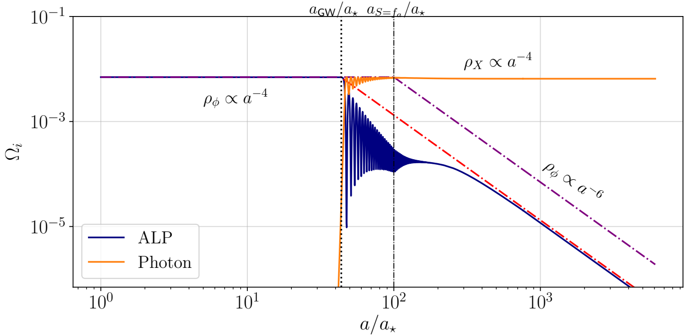

Gravitational Wave Spectrum in Kinetic Misalignment

$\Longrightarrow$ similar spectral shape as before, but with different parametric dependence:

- GW emitted around $a = a_{\mathsf{GW}}$ when X modes have grown

$$\Longrightarrow f_{\mathsf{peak}} \propto \alpha \sqrt{\frac{m_{S,0}}{f_\phi} \frac{S_i}{M_{\mathsf{Pl}}}}$$

- amplitude set by axion kinetic energy

$$\Longrightarrow \Omega_{\mathsf{GW}}^{\mathsf{peak}} \propto \frac{S_i^4}{M_{\mathsf{Pl}}^4}$$

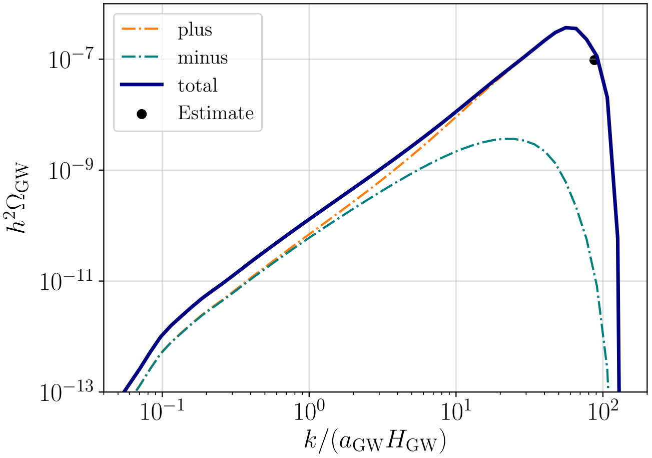

Relaxion Evolution

$$\mathcal{L} \supset -\frac{\alpha}{4}\frac{\phi}{f_\phi} X_{\mu\nu}\tilde{X}^{\mu\nu} \qquad \Longrightarrow \qquad \ddot{\phi} + 3H\dot{\phi} - \frac{\Lambda_{\text{br}}^4}{f_\phi} + \frac{\alpha}{f_\phi}\frac{\langle \tilde{X}_{\mu\nu} X^{\mu\nu}\rangle}{4\, a^4} = 0$$

- initially: $\langle \tilde{X} X \rangle$ negligible $\Longrightarrow \dot{\phi} \sim t$
- dark photon friction kicks in when $\frac{\alpha}{4a^4}\langle \tilde{X} X \rangle \sim \Lambda_{\text{br}}^4$

  $\Longrightarrow$ define time of particle production: $\left.\frac{\langle \tilde{X} X \rangle}{4a^4}\right|_{t_{\text{pp}}} = \frac{\Lambda_{\text{br}}^4}{\alpha}$
- relaxion reaches terminal velocity: $\dot{\phi} = \xi H f_\phi / \alpha$

  (ξ: $\mathcal{O}(10 - 100)$)
- relaxion stops when barriers reappear

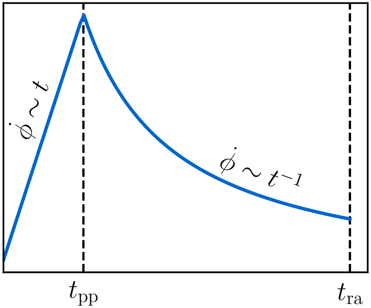

Dark Photon Production from Relaxion

dark photon EoM: $$X''_{\pm}(\tau,k) + \left(k^2 \mp k \frac{\alpha\,\phi'(\tau)}{f_\phi}\right) X_{\pm}(\tau,k) = 0$$

- $\phi' > 0 \Longrightarrow$ only '+' helicity experiences tachyonic instability
- energy predominantly transferred to most tachyonic mode: $k = \frac{\alpha\,\phi'}{2\,f_\phi} = \frac{\xi a H}{2}$
- after exiting the tachyonic band: $X(k,\tau) \propto \cos(k\tau)/\sqrt{2k}$

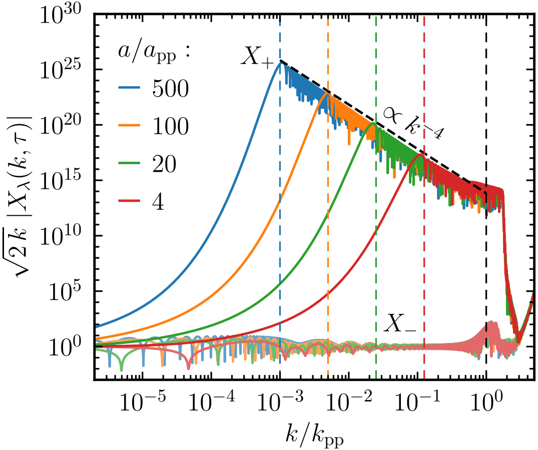

$\Longrightarrow \quad X_+(k,\tau) \sim k^{-9/2}\cos(k\tau - \xi)$ for $k > \frac{\xi}{2\tau}$

Relaxion Gravitational Wave Spectrum

- IR: $f \ll f_{\text{peak}}$

  $|\mathbf{q}| \sim |\mathbf{k}-\mathbf{q}| \sim k^X_{\text{peak}}$

  $$\Omega_{\text{GW}}(f) \sim \Omega_{\text{GW}}^{\text{peak}}\, \xi^2\, \frac{f^3}{f^3_{\text{peak}}}$$

- peak: $f \sim f_{\text{peak}}$

  $|\mathbf{q}| \sim |\mathbf{k}-\mathbf{q}| \sim k^X_{\text{peak}}$

  $$\Omega_{\text{GW}}(f_{\text{peak}}) = \Omega_{\text{GW}}^{\text{peak}}$$

- UV: $f \gg f_{\text{peak}}$

  $|\mathbf{q}| \sim k^X_{\text{peak}},\ |\mathbf{k}-\mathbf{q}| \sim k$

  $$\Omega_{\text{GW}}(f) \sim \Omega_{\text{GW}}^{\text{peak}}\, \frac{f^4_{\text{peak}}}{f^4}$$